Utilizing Chemical Looping Combustion instead of Fired-Furnace in a Steam Methane Reforming for Enhancement of Hydrogen Production in a Multi Tubular Reactor

Received: May 18, 2015/ Revised: Apr 1, 2017 / Accepted: May 7, 2017

Abstract

A novel thermally coupled reactor containing steam methane reforming in the endothermic side and chemical looping combustion as an exothermic side has been investigated in this study. In this innovative configuration, huge fired furnace of conventional steam reforming process is substituted by chemical looping combustion in a recuperative coupled reactor. This reactor has three concentric tubes where the steam methane reforming is supposed to occur in the middle tube and the inner and outer tubes are considered to be air and fuel reactors of chemical looping combustion, respectively. Copper is selected as solid oxygen carrier in the chemical looping combustion process. Both oxidation and reduction of Cu in the air and fuel reactor are exothermic and used as heat sources for endothermic steam methane reforming. A steady state heterogeneous model of fixed bed for steam reformer and a moving bed for chemical looping combustion reactor predict the performance of this new configuration. The counter-current mode is investigated and simulation results are compared with corresponding predictions of the conventional steam reformer. The results prove that synthesis gas production is increased in thermally coupled reactor in comparison with conventional steam reformer.

Keywords: Hydrogen production; Steam reforming of methane; Thermally coupled reactor; Chemical looping combustion; Cu- based oxygen carrier.

I. Introduction

Nowadays, there has been an enormous increase in energy demands due to fast growing of industrial development and population of the world. The shortage of fossil fuels as a main energy sources has brought energy crisis. In order to eliminate fossil fuels dependence, comprehensive research has been carried out on searching alternatives energy resources. Hydrogen is an excellent candidate due to its high potential energy.

1.1. Hydrogen

Hydrogen, the most common element in the earth, has been considered as an attractive energy carrier to support energy consumption. Hydrogen is an environmentally friendly, efficient, safe and sustainable energy source (Lokurlu et al., 2003; Heinzel et al., 2002). The products of hydrogen combustion are water and tiny amount of NO_x which can be reduced by proper methods. The use of hydrogen in energy sector enhances the security of energy supply and improves economic competitiveness (Muller-Langer et al., 2007). Except the nuclear fuels, hydrogen has the highest calorific value among fuels. A fuel contains higher proportion of hydrogen provides more energy (Sun et al., 2012). Therefore, pure hydrogen would be the leading fuel which can satisfy the increasing demand asked by many processes such as: methanol, electricity, ammonia, aniline, oil refining, fuel cell, vehicle engines, power plants, etc (F.Brown, 2001; Itoh et al., 2008). In fact, hydrogen is a secondary energy produced from traditional processes like: natural gas reforming, gasification of coal, electrolyses water, biomass gasification, catalytic steam reforming of natural gas, dehydrogenation of cyclic hydrocarbons, etc (Sun et al., 2012). It must be noted that hydrogen production must be low in CO_2 emissions and other pollutants. Among all mentioned technologies, catalytic steam reforming of natural gas is widely used for hydrogen production, 80-85% of the world's total hydrogen production is provided by this method (Simpson and Lutz, 2007).

1.2. Steam reforming

Steam reforming technology is the most commercial method for synthesis gas (CO, H_2) production, the hydrogen cost is less than hydrogen produced by using renewable energy sources or from gasification of solid fossil fuel (Rostrup-Nielsen, 1993; Tugnoli et al., 2008). Steam reforming may involve several catalytic steps: desulfurization of the fuel, steam reforming of methane, a water gas shift reactor and purification of hydrogen using PSA unit .This method is suitable for light hydrocarbons such as natural gas (mainly CH_4), naphtha, liquefied petroleum gas (Ryden and Lyngfelt, 2006). Three main catalytic reactions involved in steam reformer reactor are steam reforming of methane (SRM) and the water-gas shift reaction.

Conventional steam reformer consists of vertical tubes packed with Ni-based catalyst located inside huge furnace. The required heat for endothermic reforming reaction is provided by direct combustion of fuel in the furnace. Therefore, the reformer tubes are under very high thermal stress (F.Brown, 2001). In order to solve this issue, the recuperative coupled reactor has been suggested.

$$CH_4 + H_2O \leftrightarrow CO + 3H_2 \qquad \Delta H^0_{298} = -206.3 kJ/mol \quad (1)$$

$$CH_4 + 2H_2O \leftrightarrow CO_2 + 4H_2 \qquad \Delta H^0_{298} = -164.9 kJ/mol \quad (2)$$

$$CO + H_2O \leftrightarrow CO_2 + H_2 \qquad \Delta H^0_{298} = 41.1 kJ/mol \quad (3)$$

1.3. Coupled reactors

Recently, Coupling exothermic and endothermic reactions are more interested in order to improve the thermal efficiency of process and consequently enhance the production. This type of reactors aims to use energy released by exothermic reaction for proceeding endothermic reaction. In general, the coupled reactors exist into three main classes: direct coupling, recuperative coupling and finally regenerative coupling. At present, recuperative coupling has attracted the most attention of many researchers (Song et al. 2003). Hunter and McGuire (1980) were pioneers in

coupling endothermic and exothermic reactions without direct heat transfer. A review on the process intensification for methane steam reforming in a thermally coupled membrane separation technology was studied by Bhat and Sadhukhan (2009). Patel and Sunol (2007) suggested a thermally coupled membrane reactor that is composed of three channels for methane steam reforming. A numerical model for natural gas steam reforming and coupling with a furnace was developed by Ventura and Azevedo (2010). In an interesting idea, Ryden and Lyngfelt (2006) studied steam methane reforming coupled with chemical looping combustion reactor in order to enhance H_2 production with CO_2 capture. In their suggested configuration, reformer tubes are located inside the fuel reactor of chemical looping combustion. A disadvantage of their innovative configuration is erosion of reformer tubes due to harsh environment of the fuel reactor. This issue can be solved by using thermally coupled multitubular reactor which is the main goal of this study.

1.4. Chemical looping combustion

Chemical looping combustion (CLC) is a high-quality candidate which has a good potential to become an efficient technique for separating CO_2. It is easy to produce clean energy from fossil fuel by using this novel method which separates CO_2 inherently (Villa et al., 2003; Hossain and de Lasa, 2008; Zhang et al., 2009). In chemical looping combustion, a gaseous fuel like natural gas or synthesis gas is burnt with oxygen carrier which is usually a metal oxide and used to transfer oxygen from the combustion air to the fuel. Therefore fuel and combustion air never mixed and combustion products (CO_2, H_2O) do not become diluted with N_2; thus pure CO_2 is obtained after condensation of water. The process consists of two separate reactors (a fuel and an air reactor) and solid oxygen carrier transports oxygen between them, see Fig. 1 (Anheden and Svedberg, 1998; Ishida et al., 1987

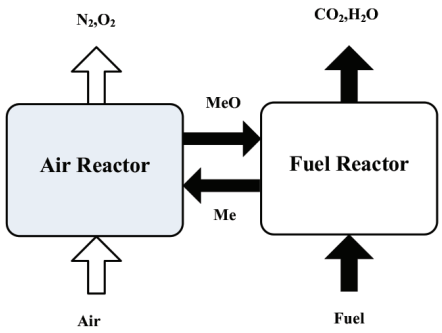

Figure 1. A schematic view of chemical looping combustion

CO_2 and H_2O exit from the fuel reactor while the outlet gas from the air reactor consists of N_2 and unused O_2. The oxygen carrier is reduced with fuel which occurs in the fuel reactor according to:

$$(2n+m)Me_xO_y + C_nH_{2m} \leftrightarrow (2n+m)Me_xO_{y-1} + mH_2O + nCO_2 \quad (4)$$

Where Me_xO_y is the common abbreviation for metal oxide in chemical looping combustion and Me_xO_{y-1} stands for the reduced oxide which is then circulated to the air reactor and oxidized according to:

$$(2n+m)Me_xO_{y-1} + \tfrac{1}{2}O_2 \leftrightarrow (2n+m)Me_xO_y \quad (5)$$

Reaction (5) is always exothermic while the amount of energy released or required in reaction (4) depended on choice of oxygen carrier. The net energy in the reactor is equal to the amount of heat released from normal combustion. That is apparent because summation of reaction (4) and (5) yields reaction (6); the conventional complete combustion of fuel.

$$C_nH_{2m} + (n+\tfrac{m}{2})O_2 \leftrightarrow mH_2O + nCO_2 \quad (6)$$

The pressure and the temperature of air and fuel reactors are 10^5Pa and 800-1200^{O}C, respectively. Up to now, researchers suggest various designs for chemical looping combustion including: moving bed, fluidized bed, packed bed and dense membrane reactor but circulating fluidized beds is common to use (Nalbandian et al., 2011; Fan et al., 2008; Son and Kim, 2006; Noorman et al., 2007). Richter and Knoche, (1983) proposed the principle of CLC process to increase the thermal efficiency in fossil fuel fired power plants for the first

time. Some years later, Lyngfelt and Leckner (1999), successfully ran a 10kW CLC prototype at Chalmers University of Technology. Choice of oxygen carriers is one of the critical steps in CLC and numbers of studies have been done on this course. An appropriate oxygen carrier has the following properties:

1) Have suitable rate of reaction both reduction and oxidation.

2) Be thermodynamically suitable to convert fully the fuel to CO_2 and H_2O.

3) Have good strength so that resistance to attrition and breakage.

4) Does not tend to agglomeration.

5) Be cheap and healthy.

6) Have high melting point.

7) Have low tendency to become deactivate with carbon and sulphur.

Based on above properties, some metal oxides like Ni, Cu, Fe, Mn could be probable oxygen carriers (Cho, 2005; Johansson, 2007; Adanez et al., 2004). In this work, Cu is used as solid particle. An advantage of chemical looping combustion compared with ordinary combustion would be the inherent capture of CO_2 from the rest of the flue gas without spending energy. (Ryden et al., 2009). Also, since indirect combustion in chemical looping combustion does not involve high temperature flame, the formation of NO_x is avoided.

1.5 Literature review

Many efforts have been done for improvement of steam methane reforming. Arab Aboosadi et al. (2011a) have considered a novel integrated thermally coupled configuration for methane steam reforming. In their simulated reactor, hydrogenation of nitrobenzene to aniline in the exothermic side is used as a heat source for endothermic reaction of steam methane reforming. The exothermic reaction takes place in the shell side and endothermic reaction occurs in the tube side. Moreover, Arab Aboosadi et al. (2011b) simulated and optimized tri-reformer (TRM) reactor for producing synthesis gas using differential evolution (DE) method. In TRM process, steam reforming, CO_2 reforming and partial oxidation of methane occurred in a single reactor. Finally, methane steam reforming and hydrogenation of nitrobenzene in hydrogen perm-selective membrane thermally coupled reactor has been optimized using differential evolution (DE) method by Rahimpour et al. (2012). Recently, Rahimpour et al. (2013) have simulated methane steam reforming technology coupled with fluidized bed chemical looping combustion using Fe- based as oxygen carrier. From previous studies, it is found that there is no modeling information available in the literature about using chemical looping combustion as a heat source for steam methane reforming in order to increase H_2 production. Therefore, it was decided to first study on this system.

1.6. Objectives

The main goal of this study is enhancement of hydrogen production theoretically in a thermally coupled steam reformer (TCSR). The endothermic and exothermic reactions are chosen the steam methane reforming and indirect combustion of methane in a chemical looping combustion process, respectively. The motivation is to combine the energy efficient concept of coupling exothermic and endothermic reactions and enhancement of hydrogen production. A steady state 1-D heterogeneous model of the thermally coupled multitubular reactor is used to estimate the performance of the proposed reactor. Ultimately, the simulation results of the TCSR were compared with the ones in conventional steam methane reforming.

2. Process description

2.1. Conventional steam reformer

Fig. 2 represents the schematic diagram of a conventional Lurgi-steam methane reformer (CR) to produce syngas for methanol synthesis process. This reactor has vertical tubes which are located inside a huge fired furnace. Natural gas is mixed with steam and entered to the steam reformer tubes as feed. Vertical tubes is packed with Ni- based catalyst, the generated heat related to natural gas combustion in burners of furnace transfers to reformer tubes (Methanol documents of Lurgi in Assaluyeh-Iran.). Table 1 shows the specification of reactor and operating conditions of the CR

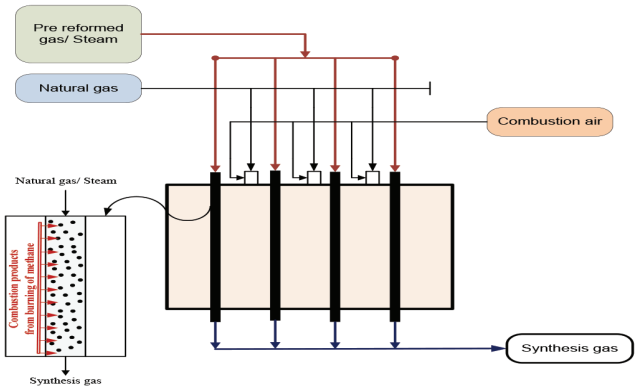

Figure 2. A schematic diagram of conventional steam methane reforming

Table 1: The specification of reactor and operating couditions

Parameter	Value	Unit
Feed composition		mol%
CO_2	1.72	[-]
CO	0.02	[-]
H_2	5.89	[-]
CH_4	32.59	[-]
N_2	1.52	[-]
H_2O	58.26	[-]
Inlet temperature	793	°K
Inlet pressure	40	bar a
Total feed gas flow	9129.6	Kmol/h
Number of tubes (in 4 rows)	184	[-]
Inside diameter	125	mm
Heated length	12	m
Catalyst volume filled in (total)	27.8	m^3
Design pressure	41	bar g
Design temperature	1063	°K
Catalyst properties		
Catalyst shape	HOLE 10 rings	
Particle size	19 ×16	mm
Void fraction	0.4	
Heat load on (tube(100% design case	68,730	Kcal/m^2h
Reformer duty (100% (design case	248.2	GJ/h
Shell side		
Combustion air		
Temperature	603	°K
Pressure	1	bar
Flow rate	114,313	sm^3/h
(Feed gas(fuel		
Temperature	307	°K
Pressure	3	bar
Flow rate	29,608	sm^3/h

2.2. Thermally coupled steam reformer (TCSR)

A conceptual schematic diagram of TCSR is shown in Fig .3. Chemical looping combustion of methane is used as exothermic reaction instead of normal combustion of natural gas in conventional steam reformer. This reactor is consisted of three concentric tubes, the inner tube is used as air reactor of CLC and the outer tube is assumed to be fuel reactor. Endothermic reaction of steam methane reforming takes place on the Ni-based catalyst counter currently in the middle tube. Air fed to the air reactor from the bottom of the reactor and natural gas combined with steam is fed to steam reformer from top of the middle reactor. A small part of steam reformer product stream recycled and combined with CH_4 to use as feed for fuel reactor. Cu as an oxygen carrier enters into air reactor of CLC from top of the reactor, moves down ward and after oxidation exits in the form of CuO from bottom of reactor. Then, copper oxide circulates in a loop and after regeneration transfers to fuel reactor and reduced with CH_4.The specific properties and operational conditions of TCSR are tabulated in Table 2. Table 1 (excluding data in the shell side) is also used for endothermic side of thermally coupled steam reformer.

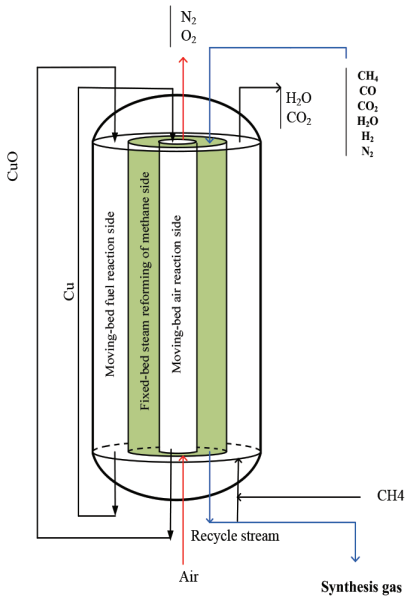

Figure 3. A conceptual schematic diagram of thermally coupled steam reformer

Table 2. The specific properties and operational conditions of TCSR

Parameter	Value
Inlet temperature of endothermic side (*K)	793
Inlet pressure of air reactor (kPa)	101.325
Inlet pressure of fuel reactor (kPa)	101.325
Inner tube or air reactor diameter (m)	0.1
Middle tube or steam reformer diameter (m)	0.1601
Outer tube or fuel reactor diameter (m)	0.1887
Length of the reactor (m)	12
Feed composition **Air reactor** (composition mol %)	
O_2	20.94
N_2	78.08
Ar	0.98
Oxygen carrier properties (CuO/Al_2O_3)	
Particle size (mm)*	0.1-0.3

Table 2. Continued...

*Porosity	0.57
*(Apparent density (kg m^{-3}	1800
*(Molar density of CuO ($molm^{-3}$	80402
*(Molar density of Cu ($molm^{-3}$	140252
(Flow rate(kg/s	0.01
Obtained from (García-Labiano * (et al., 2004	

3. Reaction scheme and kinetics

3.1. Steam methane reforming (endothermic side)

Three main reaction reactions occurred in steam reformer are steam reforming of methane and the water-gas shift reaction (Equations 1–3). The reaction rates of CR reactions proposed by Xu and Froment are as follows (Xu and Froment, 1989; Xu et al., 2002):

$$R_1 = \frac{k_1}{P_{H_2}^{2.5}}\left(P_{CH_4} P_{H_2O} - \frac{P_{H_2}^3 P_O}{K_I}\right)\times\frac{1}{\varphi^2} \quad (7)$$

$$R_2 = \frac{k_2}{P_{H_2}^{3.5}}\left(P_{CH_4} P_{H_2O}^2 - \frac{P_{H_2}^4 P_{O_2}}{K_I}\right)\times\frac{1}{\varphi^2} \quad (8)$$

$$R_3 = \frac{k_3}{P_{H_2}}\left(P_O P_{H_2O} - \frac{P_{H_2} P_O}{K_{III}}\right)\times\frac{1}{\varphi^2} \quad (9)$$

$$\varphi = 1 + K_O P_O + K_{H2} P_{H2} + K_{CH_4} P_{CH_4} + K_{H2O}\frac{P_{H2O}}{P_{H2}} \quad (10)$$

The reaction equilibrium constants and Arrhenius kinetic parameters are listed in Table 3. Table 4 shows the Van't Hoff parameters for species adsorption

3.2. Chemical looping combustion (exothermic sides)

In general, metal oxides are used as oxygen carrier in chemical looping combustion. The focus of the literature is on Ni, Cu, Fe and Mn that each one has specific advantage. In this work, Cu is selected as oxygen carrier because reduction of Cu is exothermic while for most other materials, it is endothermic.

Additionally, it is environmentally benign and reactive (Jerndal et al., 2006). The reduction and

Table 3. The reaction equilibrium constants and Arrhenius kinetic parameters for steam reforming reactions

Reaction, j	Equilibrium constant	K_{0j} $\left(\frac{mol}{kgcats}\right)$	E_j $\left(\frac{J}{mol}\right)$
1	$K_I = \exp\left(\frac{-26830}{T_s} + 30.114\right)(bar^2)$	$1.17\times10^{15}(bar^{0.5})$	240100
2	$K_{II} = K_I \cdot K_{III}(bar^2)$	$2.83\times10^{14}(bar^{0.5})$	243900
3	$K_{III} = \exp(\frac{4400}{T_s} - 4.036)$	$5.43\times10^{5}(bar^{-1})$	67130

Table 4. The Van't Hoff parameters for species adsorption

Components	$K_{0i}(bar^{-1})$	$\left(\frac{J}{mol}\right)$ ΔHi
CH_4	$10^{-4}\times6.65$	-38280
CO	$10^{-5}\times8.23$	-70650
H_2	$10^{-9}\times6.12$	-82900
H_2O	$10^{5}\times1.77$	88680
$K_{III} = \exp(\frac{4400}{T_s} - 4.036)$		

oxidation reaction of Cu in fuel and air reactor are as follows:

$$2O_2 + 4Cu \rightarrow 4CuO \qquad \Delta H^0_{1073} = -599kJ/mol \qquad (11)$$

$$4CuO + CH_4 \rightarrow CO_2 + 2H_2O + 4Cu \qquad \Delta H^0_{1073} = -202.5kJ/mol \qquad (12)$$

One of the main drawbacks of this material is its low melting point (1085°C). This makes necessary to perform at temperatures lower than its melting point in order to avoid agglomeration and loss of activity (Noorman et al. 2010). In order to describe the kinetics of metal oxide reduction and oxidation, many efforts have been done. In this way, two general types of models can be found in the literature for chemical looping combustion: one is nucleation growth model referred to as Avrami Erofeev models and the other is shrinking core models which are common method (Levenspiel, 1998; Koga and Harrison, 1984). The following equations described the unreacted shrinking core model for gas- solid reactions:

$$\frac{t}{\tau_j} = X_{s,j} \qquad \frac{dX_{s,j}}{dt} = \frac{1}{\tau_j} \qquad \tau_j = \frac{\rho_{m,i} L_i}{b_j k_j C_g^n} \tag{13}$$

Where $\rho_{m,i}$ is the molar density of reactive material in the oxygen carrier, L_i is the layer thickness of reacting solid, b_j is the stoichiometric factor in reaction j (j=oxidation, reduction), k_j is the chemical reaction rate constant in reaction j. The rate of oxidation and reduction can be calculated by following equation:

$$-r_j = \frac{\rho_{m,i}}{b_j} \frac{dX_{s,j}}{dt} \tag{14}$$

In this study, the kinetics data for the reduction and oxidation of CuO/Al_2O_3 with methane and air were used (García-Labiano et al., 2004). Table 5 shows these kinetics parameters for both oxidation and reduction reactions

Table 5. The kinetics parameters of reactions in exothermic side for Cu based oxygen carrier

Kinetic parameters	Fuel reactor	Air reactor
n	0.4	1
E $\left(\frac{kJ}{mol}\right)$	60±3	15±2
$K_0(mol^{-n}m^{3n-2}s^{-1})$	4.5×10^{-4}	4.7×10^{-6}

4. Mathematical model

Fig. 4 shows a schematic diagram for counter-current mode of the heat exchanger reactor configuration. One-dimensional homogenous model including a set of coupled mass and energy balances are taken into consideration. The hypotheses considered in the model of both exothermic and endothermic sides are summarized as follows:

- Steady state condition.
- Gas phase is considered as an ideal.
- Plug flow pattern is assumed.
- Bed porosity in axial and radial direction is constant.
- Heat loss is neglected.
- Axial diffusion of mass and heat are ignored.

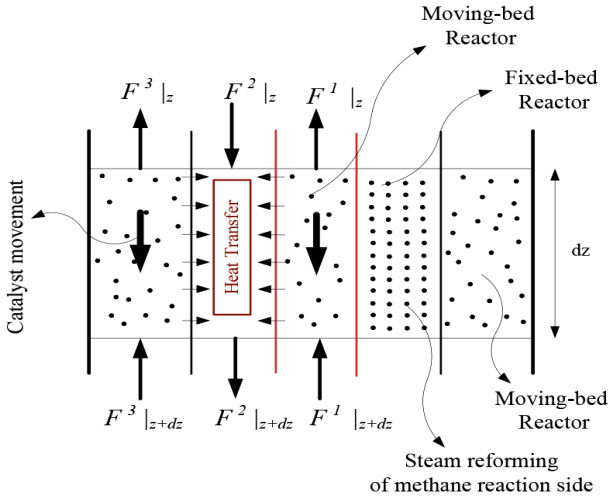

Figure 4. A schematic diagram of counter- current mode for thermally coupled steam reformer (TCSR).

4.1. Packed bed steam methane reformer tube (endothermic side)

Based on the above assumptions and considering the element with length Δz along axial direction, the differential equations describing mole and energy transfers are obtained.

The mass and energy balances for fluid and solid phases are listed in table 6.

Where T_s is temperature of steam reformer side and η is effectiveness factor defined as the ratio of the reaction rate observed on the real rate of reaction.

4.2. Moving bed chemical looping combustion (exothermic side)

There are a few investigations in the modeling of chemical looping combustion reactors. Abad et al. (2010) studied modeling of chemical looping combustion of methane using Cu-based oxygen carrier. Modeling of a 120kw chemical looping combustion reactor using Ni based oxygen carrier was introduced by kolbitch et al. (2009). Kang et al. (2010) investigated the modeling of a counter-current moving bed for fuel and steam reactors in three reactor

Table 6. Mass and energy balance and boundary conditions for solid and fluid phases in packed bed steam methane reformer tube (endothermic side).

Parameter		Value
Mass and energy balance for solid phase	$a_v ck_i^g (y_i^g - y_i^s) + r_i \rho_b = 0$	(15)
	$-\frac{c_p^g}{A}\frac{d(F_t T^g)}{dz} + a_v h_f (T_s^s - T_s^g) - \frac{\pi D_i}{A} U_f (T_s - T_f) - \frac{\pi D_i}{A} U_a (T_s - T_a) = 0$	(16)
	$a_v h_f (T_s^g - T_s^s) + \rho_b \sum_{i=1}^{N} r_i (\Delta H_{fi}) = 0$	(17)
Mass and energy balance for fluid phase	$-\frac{1}{A_a}\frac{d(F_t y_i^g)}{dz} + a_v ck_i^g (y_i^s - y_i^g) = 0$	(18)
Boundary condition	$P_j^g = P_{j0}^g \; y_{i,j}^g = y_{i0,j}^g, \; T_j^g = T_{j0}^g, \; z = 0,$	(19)

chemical looping (TRCL). Their results show that the heat transfer from oxygen carrier to gas phase is fast so that the temperature of gas and solid phases become equal along the reactor. Kang et al., 2012 suggested that a counter-current moving bed is expected to obtain high CO_2 selectivity in comparison with fluidized bed reactor. To obtain mass and energy balances in fuel and air reactor, an element with length Δz was considered. Table 7 shows the equations of mass and energy balances for fluid and solid phases for both air and fuel reactor.

Where C_p^s (J/Kg.K) is the heat capacity of the solids, F^s (kg/s) is the solid loading.

4.3 Auxiliary correlations

In order to complete the mentioned simulation equations, auxiliary correlations containing physical properties of components, mass and heat transfer coefficients should be added, see table 8.

5. Numerical solution

A governing equations of this model consists of a set of differential algebraic equations including mass balances for all sides with given boundary conditions incorporate the reaction rates as well as basic assumptions. In order to solve the set of equations, back-ward finite difference approximation was used. The reactor length is then divided into 100 separate sections and the Gauss-Newton method in MATLAB programming environment was used to solve the non-linear algebraic equations in each section. All parameters of chemical looping combustion reactors like inlet fuel reactor compositions and flow rates are determined by using trial and error method.

6. Results and Discussion

Model validation was carried out by comparing the simulated results of steam reforming side of TCSR with the observed experimental data of the industrial tubular fixed bed steam reformer reactor which is shown in Table 9. According to this table, this simulation results is in good agreement with experimental data. The simulation results of the reactor in the exothermic side are not compared with any reference case .

Table 7. Mass and energy balance and boundary conditions for solid and fluid phases in moving bed chemical looping combustion

Parameter		Value
Mass and energy balance for solid phase	$-\frac{1}{A}\frac{d(F^s y_j^s)}{dz}+\rho_b r_j b=0$	(20)
	$-\frac{cp^s}{A}\frac{d(F_t^s T_j^s)}{dz}+a_v h_f (T_j^g-T_j^s)+\rho\sum br_j(-\Delta H_{Rxn})=0$	(21)
Mass and energy balance for fluid phase	$\frac{1}{A}\frac{d(F^g y_j^g)}{dz}+\rho_b r_j=0$	(22)
	$\frac{cp^g}{A}\frac{d(F_t^g T_j^g)}{dz}+a_v h_f (T_j^s-T_j^g)+\frac{\pi D_i}{A}U(T_s^g-T_j^g)=0$	(23)
Boundary condition	$z=0; y_i^g=y_{iout}^g, y_{i0}^s=0, T^g=T_{iout}^g$	(24)

Table 8. Auxiliary correlations.

Parameter	Equation	Number
component heat capacity	$C_p=a+bT+cT^2+dT^3$	(25)
mixture heat capacity	$C_{p,mix}=\sum_{i=1}^{n} y_i \times C_{p,i}$	(26)
viscosity	$\mu=\frac{C_1 T^{C_2}}{1+\frac{C_3}{T}+\frac{C_4}{T^2}}$	(27)
overall heat transfer coefficient	$\frac{1}{U}=\frac{1}{h_i}+\frac{A_i \ln(D_o/D_i)}{2\pi K_w}+\frac{A_i}{A_o}\frac{1}{h_o}$	(28)
heat transfer coefficient between gas phase and reactor wall	$\frac{h}{C_p \rho \mu}\left(\frac{C_p \mu}{K}\right)^{2/3}=\frac{0.458}{\varepsilon_B}\left(\frac{\rho u d_p}{\mu}\right)^{-0.407}$	(29)
Pressure drop	$\frac{dP}{dz}=150\frac{(1-\varepsilon)^2 \mu u_g}{\varepsilon^3 d_p^2}+1.75\frac{(1-\varepsilon)u_g^2 \rho}{\varepsilon^3 d_p}$	(30)

Table 9. Comparison between model prediction and plant data.

Parameter	Plant	CR
Temperature (°K)	710	720.5
Composition (mol %)	Plant	CR
CO_2	5.71	5.70
CO	3.15	3.18
H_2	31.39	31.45
CH_4	20.41	20.37
N_2	1.29	1.30
H_2O	38.05	38.01
Methane conversion (%)	26.5	26.6

In this section, predicted mole fraction, pressure drop and temperature profiles in the counter current coupled reactor are presented. The results are shown in the following figures. One definition is introduced to examine the methane conversion through the reactor length:

$$\text{Methane conversion} = 100 \times \frac{F_{CH_4,in} - F_{CH_4,out}}{F_{CH_4,in}} \quad (31)$$

6.1.1. Thermal behavior

Fig. 5(a) shows the axial temperature profiles in conventional steam reformer reactor (CR) as well as the endothermic side of thermally coupled steam reformer (TCSR). As seen, the temperature profile of CR is linear while it has a curvy profile in the TCSR. Although the initial temperature of both configurations is the same, the temperature profile of TCSR is higher than that of CR as a result of distribution of solid oxygen carriers in the exothermic side which improves overall heat transfer coefficient. Since the rates of endothermic reactions are increased as temperature increases, hydrogen production is improved in TCSR. In order to make a driving force for heat transfer from exothermic side to endothermic side, the temperature of endothermic side must always lower than that of exothermic side. Fig. 5(b) represents the temperature profile of exothermic side of fuel reactor. In general, the highest temperature in thermally couple reactors is related to exothermic side where heat generation is occurring. Part of generated heat from air and fuel reactors is used for driving endothermic reaction and the rest is used to heat the reaction mixtures in three sides of TCSR. Although steam reforming is an endothermic process, its temperature increased along the reactor; it happens because the generated heat in exothermic side is so higher than consumed heat in endothermic side. The most heat transfer is occurring at the beginning of the reactor because of high temperature difference between endothermic side and exothermic sides. It is understood from Fig. 5(b) that the variation of temperature of fuel reactor is 70 K and the outlet temperature is 1160 K; fortunately, this temperature is lower than melting point of copper so that no agglomeration and loss of activity occur in the chemical looping combustion.

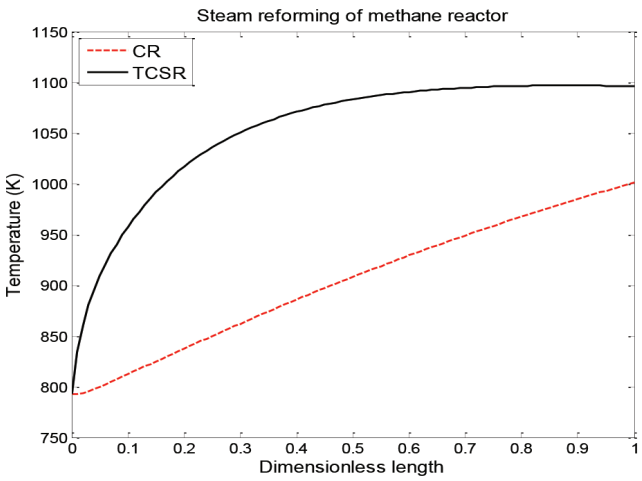

Figure 5(a). Variation of temperature for endothermic side of TCSR and CR.

6.1.2. Molar behavior

The total molar flow rate of endothermic side in CR and TCSR are compared in Fig. 6. The total molar flow rate of TCSR is higher than that of CR. The temperature profile of endothermic

side and total molar flow rate have the same trend, because these two parameters are proportional to each other (see fig 5(a)). As total molar flow rate increases, the residence time and conversion decreases.

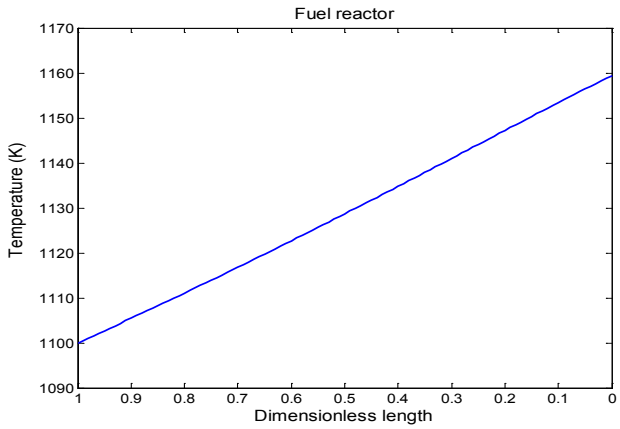

Figure 5(b). Variation of temperature for exothermic side of fuel reactor

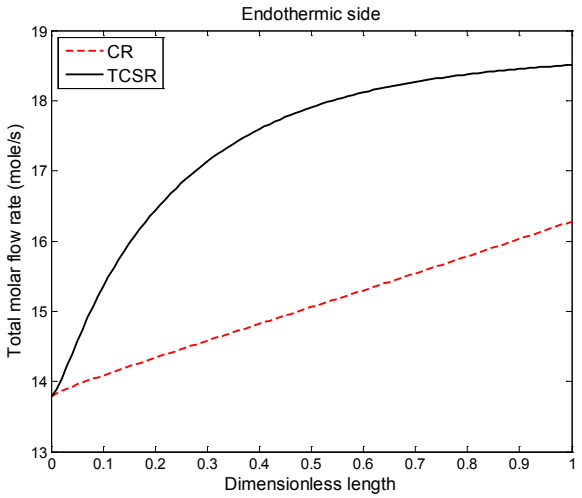

Figure 6. Comparison of total molar flow rate between endothermic sides of TCSR and CR.

Fig.7 (a)-(d) presents the comparison of mole fraction of components in endothermic side of TCSR and CR. Fig.7 (a) and (b) illustrate the mole fraction of hydrogen and carbon monoxide (CO) along the reactor at steady state. Hydrogen and CO are the most desirable products of steam reforming and fortunately their mole fractions increase in the coupled configuration in comparison with CR, because thermal effect of coupled reactor provides a good condition for heat transfer and consequently more production. The CH_4 mole fraction is depicted in Fig. 7 (c). As can be seen, the consumption rate of CH_4 as a main reactant in steam methane reforming process increases in coupled configuration. According to this figure, CH_4 conversion reaches to 52.6 % in TCSR while 26% methane conversion occurs in CR. The difference between CH_4 mole fraction profiles in CR and TCSR is owing to the temperature increase in endothermic side which causes the increase in reaction rate and CH_4 consumption. CO_2 mole fraction as an undesired product in TCSR is compared with the one in CR in Fig.7 (d). At the reactor entrance, the CO_2 mole fraction in TCSR is higher than the one in the CR configuration but at the end of reactor it becomes lower.

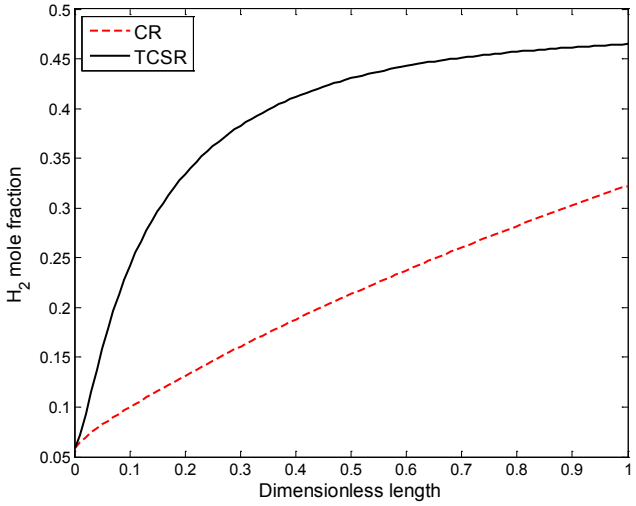

Figure 7(a). Comparison of H_2 mole fraction along the reactor axis between endothermic side of TCSR and CR.

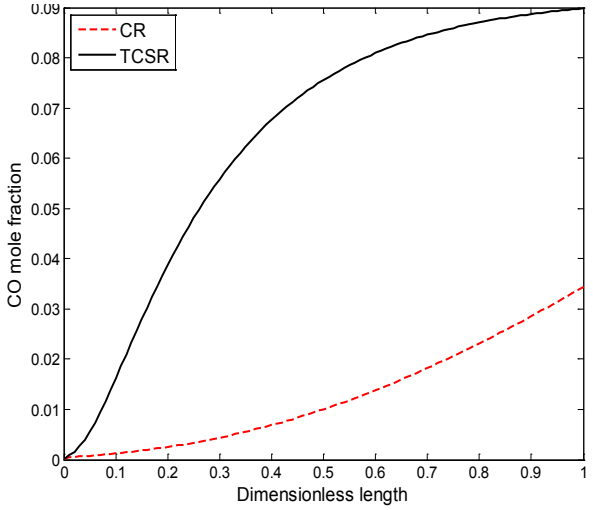

Figure 7(b). Comparison of CO mole fraction along the reactor axis between endothermic side of TCSR and CR.

Fig. 8 (a)-(c) demonstrates the mole fractions of components in exothermic side of fuel reactor. As the reaction scheme in fuel reactor shows, the mole fraction of CH_4, as reactant, decreases linearly along the fuel reactor; it is shown in Fig. 8 (a). H_2O and CO_2 are the main products of reduction reaction in fuel reactor and their mole fraction increases (see Fig 8(b) and (c)) and it can be said that all component behaviors are normal

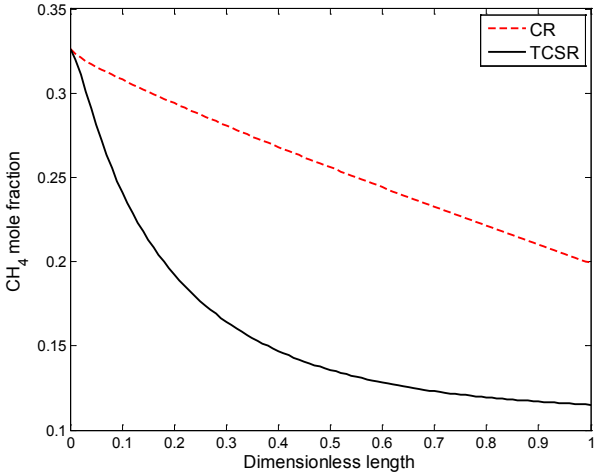

Figure 7(c). Comparison of CH_4 mole fraction along the reactor axis between endothermic side of TCSR and CR.

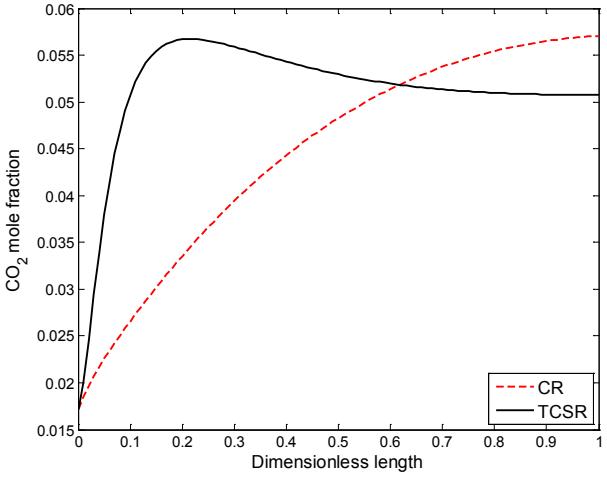

Figure 7(d). Comparison of CO_2 mole fraction along the reactor axis between endothermic side of TCSR and CR.

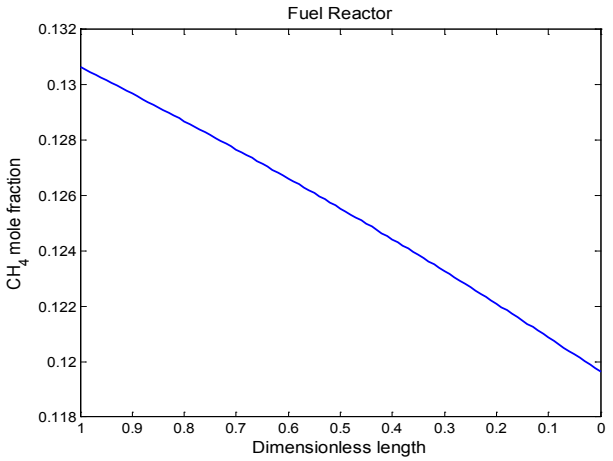

Figure 8(a). Profile of CH_4 mole fraction along the reactor axis in the fuel reactor of exothermic side in TCSR

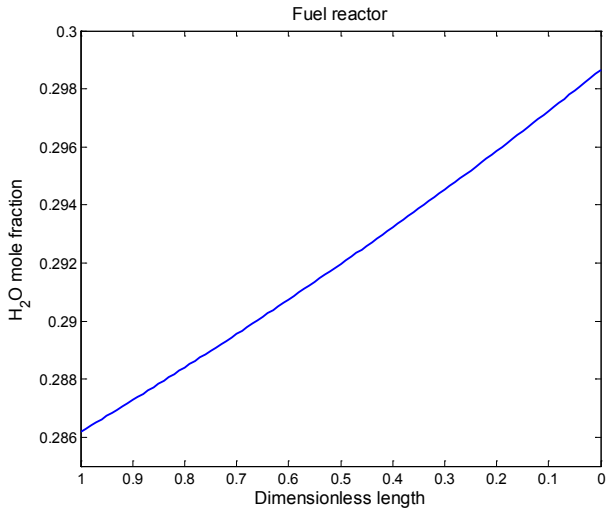

Figure 8(b). Profile of H_2O mole fraction along the reactor axis in the fuel reactor of exothermic side in TCSR

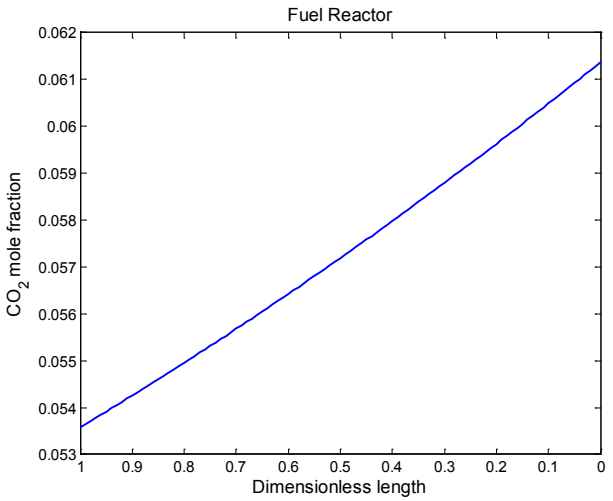

Figure 8(c). Profiles of CO_2 mole fraction along the reactor axis in the fuel reactor of exothermic side in TCSR

6.1.3. Pressure drop

Fig. 9 shows the pressure along steam methane reforming for both conventional and thermally coupled steam reformer. The Ergun Equation (which is equation (23)) usually used to calculate pressure drop through catalytic packed bed.

Since total molar flow rate and temperature profile of thermally coupled steam reformer is higher than temperature profile of conventional steam reformer, the density of gas phase and consequently the velocity and related viscose losses of TCSR become higher. As a result, pressure drop profile through this reactor is higher than conventional steam reformer.

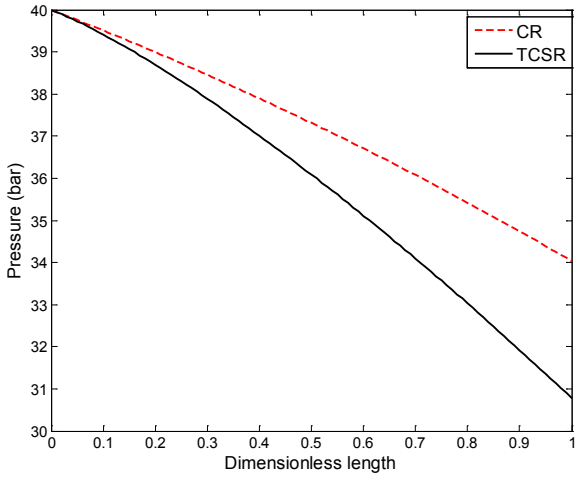

Figure 9. Pressure drop along the endothermic side CR and TCSR.

6.1.4. Influence of Inlet pressure of Methane Steam Reforming

In this section, the reactor performance is investigated for various inlet pressure of the endothermic stream. As it can be seen in Fig 10(a) and (b), by increasing the inlet pressure, the methane conversion and consequently hydrogen mole fraction in the methane steam reforming side decrease due to equilibrium related to steam reforming reactions. Fig 10 (c) shows how total molar flow rate changes with increasing inlet pressure of endothermic side. As seen, total molar flow rate decreases from 19.56 to 17.9 $\frac{mole}{s}$ because of their inverse relationship. Fig 10 (d) illustrates that the pressure drops along the reactor axis increases when the inlet pressure of endothermic stream increases from 30 to 50 bars.

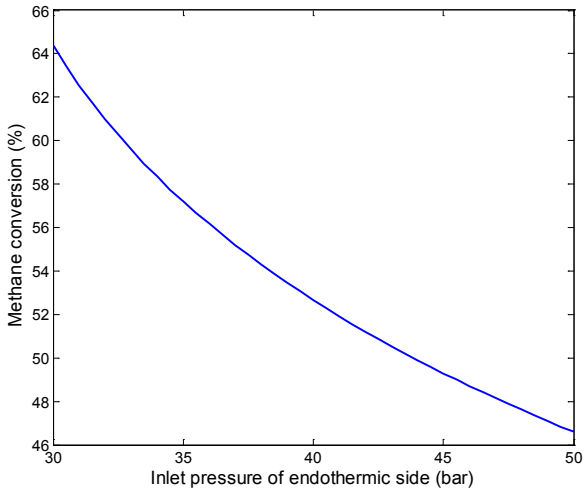

Figure 10(a). Influence of inlet pressure of endothermic stream on methane conversion along the reactor length.

7. Conclusion

Coupling endothermic reaction with an appropriate exothermic reaction improves the thermal efficiency of processes. In this study, a novel thermally coupled steam reformer has been proposed for hydrogen production by using chemical looping combustion as a heat source. Chemical looping combustion is carried out in exothermic side which consists of two moving bed reactor named as air and fuel reactors and supply the necessary heat for endothermic side. Solid metal oxide transfers oxygen between these two reactors. Copper oxide is used in this work because both reduction and oxidation of copper are exothermic.

Steam methane reforming takes place in endothermic side for hydrogen production. Thermally coupled steam reformer consists of three concentric tubes; the inner, middle and outer sides are used for air reactor, steam reformer reactor and fuel reactor, respectively. One dimensional heterogeneous model is used to simulate TCSR and comparison with conventional steam reformer. Thermal and molar behaviors of all sides as well as pressure drop profiles were investigated along the reactors. The results show that an increment

about 47% occurs in hydrogen mole fraction in TCSR compared with conventional steam reformer. In addition, the methane conversion in steam reforming reaches to 52.6%. Finally, these preliminary simulation results demonstrate that substitution of huge fired-furnace of conventional steam reformer with chemical looping combustion process is highly efficient for synthesis gas production.

Nomenclature

A_a Cross section area of each tube (m^2)

av specific surface area of catalyst pellet (m^2/m^{-3})

b Stochiometric factor for reaction in CLC

C^g Gas concentration (mol m^{-3})

cp^g Specific heat of the gas at constant pressure (j mol^{-1})

cp^s Heat capacity of oxygen carrier in CLC ($j kg^{-1}k^{-1}$)

Di Inside diameter of steam reformer (m)

F_t Total flow rate per each reaction side (mol s^{-1})

K_1 Reaction rate constant for 1st rate equation of steam reforming (mol $kg^{-1}s^{-1}$)

K_2 Reaction rate constant for 2nd rate equation of steam reforming (mol $kg^{-1}s^{-1}$)

K_3 Reaction rate constant for 3rd rate equation of steam reforming (mol $kg^{-1}s^{-1}$)

Kj Chemical reaction constant of j reaction (j=oxidation, reduction) ($mol^{1-n}m^{3n-2}s^{-1}$)

L_i Layer thickness of the reacting solid (m)

N Number of components

n Reaction order

R_1 First rate of reaction for steam reforming of CH_4 (reaction 4) (mol kg^{-1} s^{-1})

R_2 Second rate of reaction for steam reforming of CH_4 (reaction 5) (mol kg^{-1} s^{-1})

R_3 Water gas shift reactor (reaction 6) (mol kg^{-1} s^{-1})

r_j Rate of reaction occurs in chemical looping combustion based on gas phase (mol m^{-3} s^{-1})

t Reaction time (s)

T_s Bulk gas phase temperature related to steam reformer (k)

T_a Temperature of air reactor (k)

T_f Temperature of fuel reactor (k)

U_f Overall heat transfer coefficient between fuel and steam reforming reactors (W $m^{-2}k^{-1}$)

U_a Overall heat transfer coefficient between air and steam reforming reactors (W $m^{-2}k^{-1}$)

X_s Solid conversion in the chemical looping reactor

Subscripts

0 Inlet condition

a Air reactor

f Fuel reactor

g Gas phase

i Chemical species

j Oxidation, reduction

s Solid phase

Greek letters

ΔH_{fi} Enthalpy of formation of component (J mol^{-1})

ΔH_{RXn} Enthalpy of reaction (J mol^{-1})

p_b Density of catalyst bed (kg m^{-3})

ρ_{mi} Molar density of reactive material in the oxygen carrier (mol m^{-3})

η Effectiveness factor used for the intra particle transport limitation

References

1. Abad, A., Adánez, J., Garcı´a-Labiano, F., F. de Diego, L., Gayán, P., 2010. Modeling of the chemical-looping combustion of methane using a Cu-based oxygen-carrier. Combust Flame. 157, 602-15.
2. Adanez, J., F.de Diego, L., Garcia-Labiano, F., Gayan, P., Abad, A., 2004. Selection of oxygen carriers for chemical looping combustion.

Energy. Fuels. 18, 371-377.
3. (3)Anheden, M., Svedberg, G., 1998. Exergy analysis of chemical looping combustion systems. Energy. Convers. Manage. 39, 1967-1980.
4. Arab Aboosadi, Z., Rahimpour, M.R., Jahanmiri, A., 2011a. A novel integrated thermally coupled configuration for methane-steam reforming and hydrogenation of nitrobenzene to aniline. Int. J. Hydrogen. Energy. 36, 2960-2968.
5. Arab Aboosadi, Z., Jahanmiri, A.H., Rahimpour, M.R., 2011b. Optimization of tri-reformer reactor to produce synthesis gas for methanol production using differential evolution (DE) method. Appl. Energy. 88, 2691-2701.
6. Bhat, S.A., Sadhukhan, J. 2009. Process intensification aspects for steam methane reforming: an overview. AIChE J. 55,408-422.
7. Cho, P., 2005. Development and characterization of oxygen-carrier materials for chemical looping combustion. Doctoral thesis, Chalmers University of Technology, Goteborg, Sweden.
8. Fan, L., Li, F., Ramkumar, S., 2008. Utilization of chemical looping strategy in coal gasification processes. Particuology. 6, 131-142.
9. F. Brown, L., 2001. A comparative study of fuels for on-board hydrogen production for fuel-cell-powered automobiles. Int. J. Hydrogen. Energy. 26, 381-397.
10. García-Labiano, F., F.de Diego, L., Adánez, J., Abad, A., Gayán, P., 2004. Reduction and oxidation kinetics of a copper-based oxygen carrier prepared by impregnation for chemical-looping combustion. Ind. Eng. Chem .Res. 43, 8168-8177.
11. Gosiewski, K., Bartmann, U., Moszczynski, M., Mleczko, L., 1999. Effect of intraparticle transport limitations on temperature profiles and catalytic performance of the reverse-flow reactor for the partial oxidation of methane to synthesis gas. Chem. Eng. Sci. 54, 4589–602.
12. Heinzel, A., Vogel, B., Hubner, P., 2002. Reforming of natural gas-hydrogen generation for small scale stationary fuel cell systems. J. Power. Sources. 105(2), 202-7.
13. Hossain, M.M., L.de Lasa, H., 2008. Chemical looping combustion (CLC) for inherent CO2 separations- a review. Chem. Eng. Sci. 63, 4433-51.
14. Hunter, J.B., McGuire, G., 1980. Method and apparatus for catalytic heat-exchange. US Patent, 4 214 867.
15. Ishida, M., Zheng, D., Akehata, T., 1987. Evaluation of a chemical looping combustion power- generation system by graphic exergy analysis. Energy. 12, 147-154.
16. Itoh, N., Watanabe, S., Kawasoe, K., Sato, T., Tsuji, T., 2008. A membrane reactor for hydrogen storage and transport system using cyclohexane-methycyclohexane mixtures. Desalination. 234, 261-269.
17. Jerndal, E., Mattisson, T., Lyngfelt, A., 2006. Thermal analysis of chemical-looping combustion. Chem. Eng. Res. Des. 84, 795-806.
18. Johansson, M., 2007. Screening of oxygen-carrier particles based on iron-, manganese-, copper-, nickel oxides for use in chemical looping technologies. Doctoral thesis, Chalmers University of Technology, Goteborg, Sweden.
19. Kang K.S., Kim C.H., Bae K.K., Cho W.C., Jeong, S.U., Kim, S.H., Park, C.S., 2012. Modeling a counter-current moving bed for fuel and steam reactors in the TRCL process. Int. J. Hydrogen. Energy. 37, 3251-3260.
20. Kang K.S., Kim C.H., Bae K.K, Cho W.C, Kim S.H, Park C.S., 2010. Oxygen-carrier selection and thermal analysis of the chemical-looping process for hydrogen production. Int. J. Hydrogen. Energy. 35, 12246-54.
21. Koga, Y., Harrison, L.G., 1984. In: Bamford C.H, Tipper C.F.H, Compton R.G. (Eds.), Comprehensive chemical kinetics. Elsevier, Amsterdam. 21, 120.
22. Kolbitsch, P., Pröll, T., Hofbauer, H., 2009. Modeling of a 120 kW chemical looping combustion reactor system using a Ni-based oxygen carrier. Chem. Eng. Sci. 64, 99 –108.
23. Levenspiel, O., 1998. Chemical reaction engineering. John wiley and sons, New York.
24. Lokurlu, A., Grube, T., Hohlein, B., Stolten, D., 2003. Fuel cells for mobile and stationary applications- cost analysis for combined heat and power stations on the basis of fuel cells. Int. J. Hydrogen. Energy. 28(7), 703-11.
25. Lyngfelt, A., Leckner, B., 1999. Technologies for CO_2 separation. In minisymposium on CO_2 capture and storage. Goteborg: Chalmers University of Technology and University of

Gothenburge.
26. Muller-Langer, F., Tzimas, E., Kaltschmidtt, M., Peteves, S., 2007. Techno-economic assessment of hydrogen production processes for the hydrogen economy for the short and medium term. Int. J. Hydrogen. Energy. 32, 3797-810.
27. Nalbandian, L., Evdou, A., Zaspalis, V., 2011. La1-x Srx MyFe1-yO3-s perovskites as oxygen-carrier materials for chemical-looping reforming. Int. J. Hydrogen. Energy. 36, 6657-6670.
28. Noorman, S., van Sint Annaland, M., Kuipers, H, 2007. Packed bed reactor technology for chemical-looping combustion. Ind. Eng. Chem. Res. 46, 4212-4220.
29. Noorman, S., van Sint Annaland, M., Kuipers, J.A.M., 2010. Experimental validation of paced bed chemical-looping combustion. Chem. Eng. Sci. 65, 92-97.
30. Patel, K.S., Sunol, A.K., 2007. Modeling and simulation of methane steam reforming in a thermally coupled membrane reactor. Int. J. Hydrogen. Energy.32, 2344-58.
31. Rahimpour, M.R., Arab Aboosadi, Z., Jahanmiri, A.H., 2012. Differential evolution (DE) strategy for optimization of methane steam reforming and hydrogenation of nitrobenzene in a hydrogen perm-selective membrane thermally coupled reactor. Int. J. Energy. Res. DOI: 10.1002/er.2887.
32. rahimpour, m.r., hesami, m., saidi, m., jahanmiri a., farniaei m., abbasi m., 2013. methane steam reforming thermally coupled with fuel combustion: application of chemical looping concept as a novel technology. energy & fuel. 27, 2351-2362.
33. Richter, H.J., Knoche, K.F., 1983. Reversibility of combustion process. In: Gaggioli R.A, editor. Efficiency and costing, second law analysis of process. ACS Symposium Series. Washington DC. pp.71-85
34. Rostrup-Nielsen J.R., 1993. Production of synthesis gas. Catal. Today. 18,305-324.
35. Ryden, M., Cleverstam, E., Lyngfelt, A., Mattisson, T., 2009. Waste products from the steel industry with NiO as additive as oxygen carrier for chemical looping combustion. Int. J. Greenhouse. Gas. Control. 3, 693-703.
36. Ryden, M., Lyngfelt, A., 2006. Using steam reforming to produce hydrogen with carbon dioxide capture by chemical-looping combustion. Int. J. Hydrogen. Energy. 31, 1271-1283.
37. Ryden, M., Lyngfelt, A., Mattisson, T., 2006. Two novel approaches for hydrogen production; chemical-looping reforming and steam reforming with carbon dioxide capture by chemical looping combustion. WHEC. 16, 13-16.
38. Simpson, A.P., Lutz A.E., 2007. Exergy analysis of hydrogen production via steam methane reforming. Int. J. Hydrogen. Energy. 32, 4811-20.
39. Song, K.S., Seo Y.S., Yoon, H.Y., Cho, S.J., 2003. Characteristics of the NiO/Hexaaluminate for chemical looping combustion. Korean. J. Chem. Eng. 20, 471-5.
40. Son, S.R., Kim, S.D., 2006. Chemical looping combustion with NiO and Fe_2O_3 in a thermo balance and circulating fluidized bed reactor with double loops. Ind. Eng. Chem. Res. 45(8), 2689-2696.
41. Sun, Z., Liu, F., Lin, X., Sun, B., Sun, D., 2012. Research and development of hydrogen fueled engines in china. Int. J. Hydrogen. Energy. 37, 664-681.
42. Tugnoli, A., Landucci, G., Cozzani, V., 2008. Sustainability assessment of hydrogen production by steam reforming. Int. J. Hydrogen. Energy. 33, 4345-57.
43. Villa, R., Cristiani, C., Groppi, G., Lietti, L., Forzatti, P., Cornaro, U., Rossini, S., 2003. Ni based mixed oxide materials for CH4 oxidation under redox cycle conditions. J. Mol. Catal. A: Chem. 204-205, 637–646.
44. Ventura, C., Azevedo, J.L.T. 2010. Development of a numerical model for natural gas steam reforming and coupling with a furnace model. Int. J. Hydrogen. Energy. 35,9776-87.
45. Xu, G., Li, P., Rodrigues, A., 2002. Sorption enhanced reaction process with reactive regeneration. Chem. Eng. Sci. 57, 3893-908.
46. Xu, J., Froment, G., 1989. Methane steam reforming, methanation and water gas shift: I. Intrinsic kinetics. AIChE. J. 35, 88-96.
47. Zhang, X., Han, W., Hong, H., Jin, H., 2009. A chemical intercooling gas turbine cycle with chemical-looping combustion. Energy. 34, 2131-2136.

جایگزینی چرخه شیمیایی احتراق به جای کوره در فرآیند تبدیل بخار با استفاده از کاتالیست مس

چکیـــــــده

این مقاله، به بررسی مدل سازی راکتور کوپلینگ حرارتی دو واکنش کاتالیستی ریفرمینگ متان با بخارآب و چرخه شیمیایی احتراق جهت بهبود میزان تولید هیدروژن می پردازد. کوپلینگ حرارتی دو واکنش گرماگیر و گرماده باعث بهبود بازده حرارتی و در نتیجه افزایش میزان تولید میشود. ریفرمینگ متان با بخارآب فرآیندی گرماگیر است که گرمای آن توسط یک کوره فراهم می شود. در این حالت، لوله های ریفرمرتحت تنش حرارتی بالایی قرار دارند. با جایگزینی این کوره با چرخه شیمیایی احتراق برانیم تا علاوه بر حل این مشکل تولید هیدروژن را در یک فرآیند کوپلینگ افزایش دهیم. چرخه شیمیایی احتراق نوعی احتراق غیر مستقیم است که از دو راکتور هوا و سوخت تشکیل شده است. در این فرآیند از تماس مستقیم سوخت با اکسیژن جلوگیری می شود و شرایط برای واکنش سوخت با یک اکسید فلز فراهم می شود. کوپل این دو واکنش کاتالیستی در یک راکتور سه لوله هم مرکز انجام می شود. راکتور درونی و بیرونی به ترتیب به عنوان راکتورهای هوا و سوخت چرخه شیمیایی احتراق و راکتور میانی راکتور ریفرمینگ متان منظور می شود. راکتور چرخه شیمیایی احتراق بستر متحرک است که مس در آن کاتالیست متحرک است. راکتور ریفرمینگ متان بستر ثابت است که از کاتالیست نیکل پر شده است. شبیه سازی فرآیند با استفاده از یک مدل یک بعدی هتروژن انجام شد. صحت مدل انجام شده با داده های راکتورریفرمینگ متان پالایشگاه گاز زاگرس عسلویه بررسی شد. نتایج حاصل با موارد مشابه در راکتور معمولی ریفرمینگ متان مقایسه شد که افزایش چشمگیر میزان هیدروژن مشاهده شد.

واژگان کلیدی: تولید هیدروژن، ریفرمینگ متان با بخارآب، چرخه شیمیایی احتراق ، کاتالیست نیکل و مس